



Nanoscale Proximity Effect in the High-Temperature Superconductor $\text{Bi}_2\text{Sr}_2\text{CaCu}_2\text{O}_{8+\delta}$ Using a Scanning Tunneling Microscope

Colin V. Parker,¹ Aakash Pushp,^{1,2} Abhay N. Pasupathy,¹ Kenjiro K. Gomes,^{1,*} Jinsheng Wen,³ Zhijun Xu,³ Shimpei Ono,⁴ Genda Gu,³ and Ali Yazdani¹

¹Joseph Henry Laboratories and Department of Physics, Princeton University, Princeton, New Jersey 08544, USA

²Department of Physics, University of Illinois at Urbana-Champaign, Urbana, Illinois 61801, USA

³Condensed Matter Physics and Materials Science, Brookhaven National Laboratory (BNL), Upton, New York 11973, USA

⁴Central Research Institute of Electric Power Industry, Komae, Tokyo 201-8511, Japan

(Received 16 November 2009; published 15 March 2010)

High-temperature cuprate superconductors exhibit extremely local nanoscale phenomena and strong sensitivity to doping. While other experiments have looked at nanoscale interfaces between layers of different dopings, we focus on the interplay between naturally inhomogeneous nanoscale regions. Using scanning tunneling microscopy to carefully track the same region of the sample as a function of temperature, we show that regions with weak superconductivity can persist to elevated temperatures if bordered by regions of strong superconductivity. This suggests that it may be possible to increase the maximum possible transition temperature by controlling the distribution of dopants.

DOI: 10.1103/PhysRevLett.104.117001

PACS numbers: 74.72.-h, 74.45.+c, 74.78.Na

Many properties of high-temperature cuprate superconductors, such as the transition temperature T_c and the presence of pseudogap, have a strong doping dependence. What happens when two regions with different doping are put into contact? Since pairing in cuprate superconductors has a very local character [1–4], one expects the coherence length to be short, and any proximity effects to occur only on microscopic length scales. Nonetheless, some experiments have demonstrated that high- T_c Josephson junctions can be made with thicknesses many times the coherence length [5]. Other experiments on bilayers have shown transition temperatures higher than that of either layer in isolation [6–8]. Microscopic theories to explain these phenomena include Josephson coupling between superconducting islands [9] and enhancement of the phase stiffness in underdoped regions by proximity to overdoped regions [7,10,11]. Such scenarios are inherently interesting due to the possibility that interface superconductivity can occur at temperatures above the maximum possible in bulk samples. To date no experiments have been performed to investigate proximity effects locally at microscopic length scales. Here we report a proximity effect in the cuprate superconductor $\text{Bi}_2\text{Sr}_2\text{CaCu}_2\text{O}_{8+\delta}$ using STM and the intrinsic nanoscale spatial variation of the sample. We show that indeed patches of the sample with weaker superconductivity can be enhanced if surrounded by patches with stronger superconductivity, demonstrating that the collapse of superconductivity is caused by more than local thermal pair breaking.

Our experiments were performed in a compact variable temperature STM, with the unique ability to acquire spectroscopy on nearly identical grids of points over a wide range of temperatures. This allows us to perform spatial correlations using data from multiple temperatures. The

pairing gap is measured from the local differential conductance (dI/dV), which is proportional to the local density of states. Figure 1 shows a representative dI/dV spectrum for the high-temperature superconductor $\text{Bi}_2\text{Sr}_2\text{CaCu}_2\text{O}_{8+\delta}$ (Bi-2212). At 30 K there is a visible gap in the spectrum, by 70 K it has diminished considerably, and by 78 K it is gone completely. The gap has been previously described by a d -wave extension to the BCS theory with the addition of a lifetime broadening term [12,13].

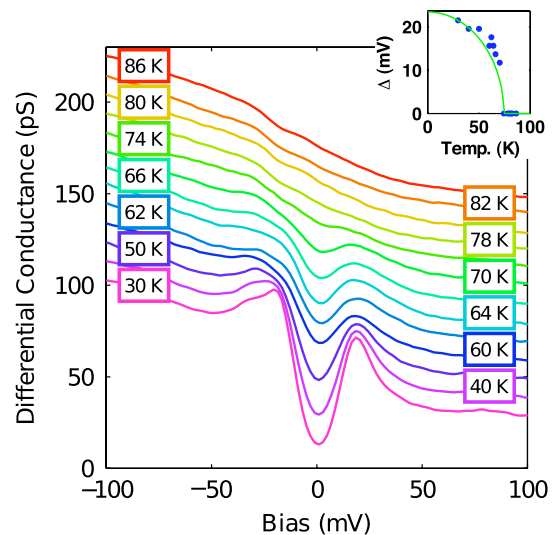


FIG. 1 (color online). Representative dI/dV spectrum at the same point at different temperatures. The setpoint was at -200 mV. The evolution of the spectrum shows a gap that closes near 74 K (T_c is 65 K). The inset shows the gap as extracted from the peak location as a function of temperature.

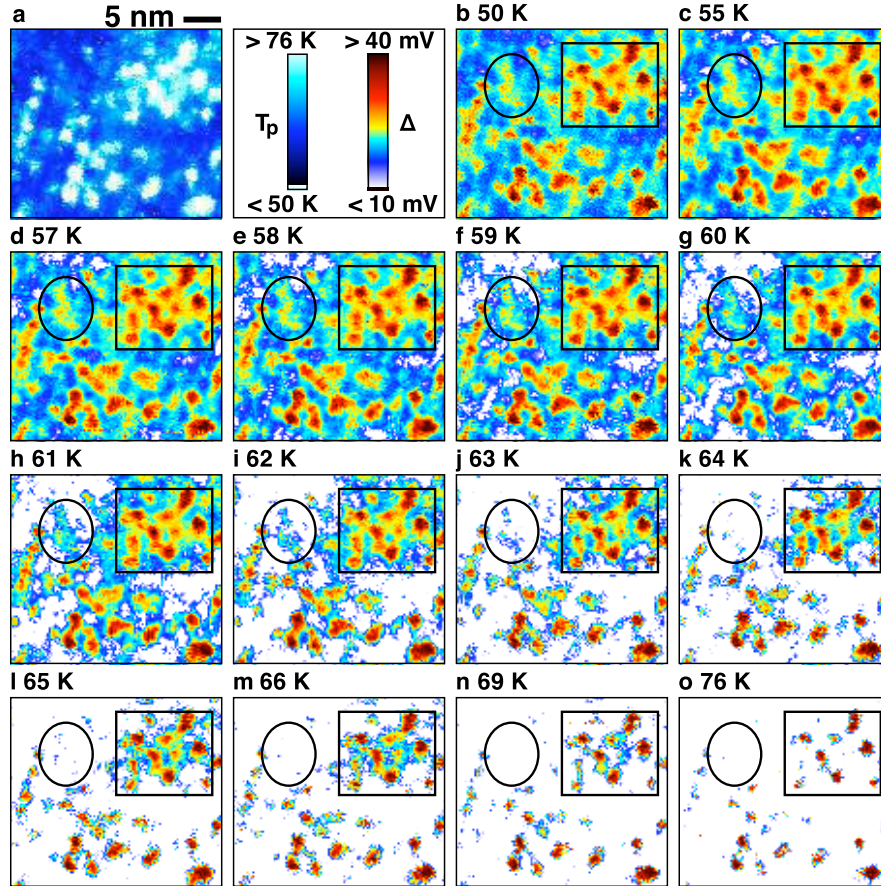


FIG. 2 (color online). Evolution of the gap distribution with temperature. (a) Map of the local pairing temperature (T_p). The pairing temperature is determined from the sequence of images in (b)–(o) by finding the temperature above which there is no maximum in the conductance on the positive bias side. (b)–(o) A 25×28 nm “gap map” taken at several different temperatures showing the distribution of gaps in real space. At each temperature, the gap map has been aligned to allow point-by-point comparison between maps.

For high-temperature cuprate superconductors, the superconducting gap varies from smallest to largest by a factor of 2 on nanometer scales [1–4]. By identifying the same atoms in the topography at multiple temperatures we are able to measure dI/dV spectra for the same point at different temperatures. Recently, we have used this technique to visualize the development of superconductivity on the atomic scale in Bi-2212. We have found that the temperature dependence of the spectroscopic gap $[\Delta(r, T)]$ is inhomogeneous, and that the gap vanishes at a local temperature $T_p(r)$, which is positively correlated in space with the gap size [1]. Furthermore, the spectroscopic gap below T_c is spatially correlated to the density of states at the Fermi level well above T_c where the gap is absent [12]. For this work we simplify the analysis of a large number of points by using a simple, operational definition for the gap and the pairing temperature. We follow the definition used previously [1,2], defining the gap value as the point of maximum differential conductance for positive bias. This simple procedure agrees with more elaborate fitting schemes to within 10% in most cases. We also need a simple method to describe the temperature evolution of

the gap. For this, we define the pairing temperature T_p , which is the highest temperature at which a maximum in the dI/dV spectrum can be observed within experimental resolution at positive bias.

In underdoped samples, multiple energy features are present in STM spectroscopy [1]. While high energy features survive to temperatures well above T_c , lower energy features show the closing of a nodal gap near T_c [14,15]. However, for strongly overdoped samples pseudogap behavior is absent, there is only one spectroscopic feature in tunneling data, and the median value of T_p is near the resistive transition temperature T_c . Furthermore, an inhomogeneous superconducting transition is supported by Nernst measurements [16] and muon spin resonance [17]. Therefore, Δ may be taken as the superconducting gap, and T_p as the temperature for the onset of pairing. We have done detailed measurements of the local T_p and the local Δ for a grid of points on an overdoped sample of Bi-2212 with $T_c = 65$ K, for a range of temperatures from 50 to 76 K. These measurements provided evidence that nanoscale regions distinguished by inhomogeneity can influence each other via the proximity effect. We show that the

fractional variation in T_p is less than that for Δ . The pairing order parameter in a disordered sample has been analyzed theoretically at low temperature [18,19] and near the transition [20], but a direct comparison of spatial variation between T_p and Δ was not made. Our measurements show that the length scale for correlations in T_p is longer by 20% than the length scale for the gap. Furthermore, we find that the local gap can disappear at distinct temperatures for different spatial positions on the sample, even if these positions have the same magnitude of gap at low temperature, and this anomalous temperature evolution of the local gap is influenced by the size of gaps in the surrounding 1 nm region.

We have the spectral evolution for more than 10 000 points in a 25×28 nm grid [21] at 14 different temperatures from 50 to 76 K. For each temperature, we can determine the gap at each point, and plot a series of “gap maps,” or 2D false color images showing the spatial distribution of gaps, shown in Figs. 2(b)–2(o). Using simultaneously recorded topographic information, we can align gap maps taken at different temperatures, despite their being taken over slightly different areas with varying amounts of thermal drift and piezocreep. This is accomplished by interpolating the two dimensional data in order to maximize the agreement between temperatures. To avoid biasing the results all alignment is based exclusively on topographic data. Points with median-sized gaps surrounded by large gapped regions (consider points with gaps near 20 mV within the box in the upper right-hand of the panels of Fig. 2) survive to higher temperatures than regions with similar absolute gap sizes elsewhere (consider the oval shaped region in the upper left), which supports our main claim. From the data of Figs. 2(b)–2(o), we can determine T_p for each point, restricted to the temperature range for which we have data, so that we can test our claims statistically. Figure 2(a) shows the spatial distribution of T_p . This is well correlated to the low temperature gap value from Fig. 2(b), as we expect if the temperature evolution is determined locally. Figure 3(a) shows a histogram of all measured gaps and their corresponding T_p values, confirming that the two quantities are well correlated (81%). If we use the median value of the gap (20 mV) and the median value of T_p (64 K), we obtain $2\Delta/k_B T_p = 7.4$ [the straight green line in Fig. 3(a)], consistent with previous work [1]. By choosing bins of gap size and averaging the T_p values in each bin, we can establish a more detailed relation between Δ and T_p [the curved red line in Fig. 3(a)]. The slope of the distribution is significantly shallower than the linear relation $2\Delta/k_B T_p = 7.4$. That is, the relative variation of Δ is greater than that for T_p . Indeed, this is quite a significant effect, as it means that, for example, 17 mV gaps will survive, on average, to temperatures 6 K above where one would expect based on a linear relation. We take this as evidence that T_p is determined not only by the local gap, but also by the gap in the surrounding region. Therefore, the variation in T_p will

be reduced, as this quantity is spatially averaged over some window.

We have found direct evidence that the temperature evolution can be more accurately predicted given knowledge of the gap in the vicinity of a point, compared with knowledge of the gap at a single point only. One can clearly see from Fig. 3(a) that knowledge of the gap can only determine T_p in a statistical way; that is, different points of equal gap size have measurably different values of T_p . If the pairing temperature were to depend only locally on the gap, the distribution of T_p values with the same gap would only be due to random fluctuations. Therefore, when we subtract the mean T_p value (based on gap size) from each measured T_p value, the result should be uncorrelated noise. However, Fig. 3(b) shows a significant spatial pattern associated with this quantity, which we call δT_p .

We can understand the meaning of δT_p and relate it to the gap map using the cross correlation as a function of separation distance. We define the cross correlation as

$$\rho(\mathbf{x}) = \frac{1}{N\sigma_{\delta T_p}\sigma_{\Delta}} \sum_{\mathbf{y}} \delta T_p(\mathbf{y})\Delta(\mathbf{y} - \mathbf{x}), \quad (1)$$

where $\sigma_{\delta T_p}$ and σ_{Δ} are the standard deviations of δT_p and Δ , respectively, and \mathbf{y} runs over the N available data points. Although the supermodulation on the b axis does have a small correlation with the gap, in practice ρ is isotropic within the noise, so we plot a circular average in Fig. 4. For zero separation, the cross correlations mathematically must be zero, because we have explicitly eliminated the local relation between Δ and T_p when we subtract the mean to produce δT_p . The peak at positive separation indicates that T_p at a particular point is significantly determined by gaps 1 nm away, which we attribute to the proximity effect. In addition, there is a long tail of positive correlation, indicating that T_p is also dependent on gaps

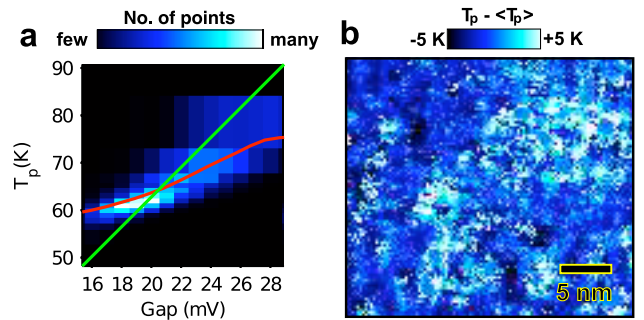


FIG. 3 (color online). Relation between Δ and T_p . (a) Two dimensional histogram of Δ and T_p values, showing the strong correlation. The straight green line represents the linear relation $2\Delta/k_B T_p = 7.4$, which is determined from the median values of Δ and T_p . The curved red line represents the average value of T_p as a function of Δ . (b) The deviation in T_p from the average, that is, $\delta T_p = T_p - \langle T_p \rangle$, where $\langle T_p \rangle$ is the average T_p for gaps with the same size.

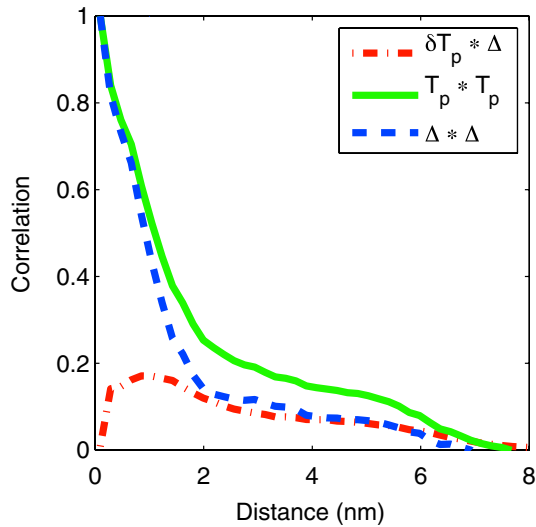


FIG. 4 (color online). Correlation length scales. The cross correlation between δT_p and Δ as a function of separation, and the autocorrelations of Δ and T_p , radially averaged. The cross correlation shows that areas with large T_p values for their gap size are on average surrounded by larger gap regions. The autocorrelations show that T_p has stronger correlation on length scales above 1 nm. The results are not significantly different if averaged along the a or b axis instead of radially.

several nanometers away. Figure 4 also shows the autocorrelation of Δ and T_p averaged along both axes and plotted as a function of separation, showing that the pairing temperature has a longer length scale (1.1 nm at half maximum) than the gap (0.9 nm at half maximum). These correlations occur on length scales longer enough than the 0.25 nm pixel spacing to rule out “smoothing” due to the interpolation used in aligning between different temperatures. The strength of T_p correlations is also higher than that of gap correlations over the tail of the distribution (1–6 nm). Although the exact shape of this tail may reflect details of the specific area chosen for study, the fact that the T_p correlation is consistently higher and the $\delta T_p - \Delta$ cross correlation also extends to this distance indicates that the process by which the gap collapses is more sensitive to the surrounding several nanometers than the process that sets the gap energy scale.

We have performed the first detailed measurements of the temperature evolution of the superconducting gap for a large number of points in overdoped $\text{Bi}_2\text{Sr}_2\text{CaCu}_2\text{O}_{8+\delta}$. Because of dopants and crystalline disorder, the tendency toward pairing is naturally inhomogeneous. Correspondingly, the superconducting gap is also inhomogeneous, albeit smoothed out by interactions between regions. The temperature evolution is also inhomogeneous, but we have found that compared to the gap the magnitude of its variation is more and the length scale of its variation is shorter; that is, the temperature evolution is even more smoothed out. Also, regions of the sample with a small

gap magnitude can have this gap survive to higher temperatures if surrounded by larger gapped regions. We speculate that the closing of the gap may have to do not just with thermal pair breaking, but also with phase fluctuations, so that regions bordered by larger gapped regions have the phase pinned up to a higher temperature than similar regions bordered by small gapped regions.

*Current Address: Department of Physics, Stanford University, Stanford, CA 94305, USA.

- [1] K. K. Gomes, A. N. Pasupathy, A. Pushp, S. Ono, Y. Ando, and A. Yazdani, *Nature (London)* **447**, 569 (2007).
- [2] C. Howald, P. Fournier, and A. Kapitulnik, *Phys. Rev. B* **64**, 100504(R) (2001).
- [3] S. H. Pan *et al.*, *Nature (London)* **413**, 282 (2001).
- [4] K. McElroy, J. Lee, J. Slezak, D. Lee, H. Eisaki, S. Uchida, and J. Davis, *Science* **309**, 1048 (2005).
- [5] I. Bozovic, G. Logvenov, M. A. J. Verhoeven, P. Caputo, E. Goldobin, and M. R. Beasley, *Phys. Rev. Lett.* **93**, 157002 (2004).
- [6] O. Yuli, I. Asulin, O. Millo, D. Orgad, L. Iomin, and G. Koren, *Phys. Rev. Lett.* **101**, 057005 (2008).
- [7] E. Berg, D. Orgad, and S. A. Kivelson, *Phys. Rev. B* **78**, 094509 (2008).
- [8] A. Gozar, G. Logvenov, L. F. Kourkoutis, A. T. Bollinger, L. A. Giannuzzi, D. A. Muller, and I. Bozovic, *Nature (London)* **455**, 782 (2008).
- [9] V. Kresin, Y. Ovchinnikov, and S. Wolf, *Phys. Rep.* **431**, 231 (2006).
- [10] S. Okamoto and T. A. Maier, *Phys. Rev. Lett.* **101**, 156401 (2008).
- [11] L. Goren and E. Altman, *Phys. Rev. B* **79**, 174509 (2009).
- [12] A. Pasupathy, A. Pushp, K. Gomes, C. Parker, J. Wen, Z. Xu, G. Gu, S. Ono, Y. Ando, and A. Yazdani, *Science* **320**, 196 (2008).
- [13] J. W. Alldredge *et al.*, *Nature Phys.* **4**, 319 (2008).
- [14] M. C. Boyer, W. D. Wise, K. Chatterjee, M. Yi, T. Kondo, T. Takeuchi, H. Ikuta, and E. W. Hudson, *Nature Phys.* **3**, 802 (2007).
- [15] A. Pushp, C. Parker, A. Pasupathy, K. Gomes, S. Ono, J. Wen, Z. Xu, G. Gu, and A. Yazdani, *Science* **324**, 1689 (2009).
- [16] Y. Wang, L. Li, and N. P. Ong, *Phys. Rev. B* **73**, 024510 (2006).
- [17] J. E. Sonier, M. Ilton, V. Pacradouni, C. V. Kaiser, S. A. Sabok-Sayr, Y. Ando, S. Komiya, W. N. Hardy, D. A. Bonn, R. Liang, and W. A. Atkinson, *Phys. Rev. Lett.* **101**, 117001 (2008).
- [18] A. C. Fang, L. Capriotti, D. J. Scalapino, S. A. Kivelson, N. Kaneko, M. Greven, and A. Kapitulnik, *Phys. Rev. Lett.* **96**, 017007 (2006).
- [19] A. V. Balatsky, I. Vekhter, and J.-X. Zhu, *Rev. Mod. Phys.* **78**, 373 (2006).
- [20] B. M. Andersen, A. Melikyan, T. S. Nunner, and P. J. Hirschfeld, *Phys. Rev. B* **74**, 060501 (2006).
- [21] These data are taken in the same area of the same sample as used in Ref. [12].